Engineering Solid Mechanics 14 (2026) 117-126

Contents lists available at GrowingScience

Engineering Solid Mechanics

homepage: www.GrowingScience.com/esm

Investigating interfacial fracture in alumina/silver bimaterial: A study of stress intensity factors and material behavior under mechanical, thermal, and thermo-mechanical loads

Lamisse Tayeboun[a*], Souad Sellam[a], Hamida Fekirini[a], Farida Bouafia[a,b]

[a]*LMPM, Mechanical Engineering Department, University of Sidi Bel Abbes, Sidi Bel Abbes 22000, Algeria*
[b]*University of Ain Temouchent, Mechanical Engineering Department, Ain Temouchent 46000, Algeria*

ARTICLEINFO

Article history:
Received 10 May 2025
Accepted 11 October 2025
Available online
11 October 2025

Keywords:
Bimaterials, Interface
Crack
Failure
Stress intensity factor
Mechanical and Thermal load

ABSTRACT

This study investigates the fracture behavior of bimaterials, specifically focusing on the Alumina/Silver interface under mechanical, thermal, and thermo-mechanical loading conditions. Through the analysis of Stress Intensity Factors (SIFs) across various crack lengths, temperatures, and along multiple regions and fronts of the crack, we provide valuable insights into the distribution and the nature of stresses, shedding light on how different loading conditions influence crack propagation. Our findings show that, under mechanical loading, the tensile mode SIF (K_I) exhibits a straightforward relationship with applied stress, increasing with crack length. In contrast, under thermal loading, K_I generally decreases on the surface as the temperature rises, while it increases within the interface, highlighting the complex interplay of thermal expansion and the mismatch of material properties. The thermo-mechanical case combines these effects, further amplifying the role of residual stresses from manufacturing processes and thermal stresses, significantly affecting SIFs and crack growth, especially in bimaterial interfaces. These results contribute to a deeper understanding of fracture mechanisms in hybrid materials.

© 2026 Growing Science Ltd. All rights reserved.

1. Introduction

Fracture mechanisms in materials are critical to understanding their failure behavior under various loading conditions. Generally, the fracture process can be divided into two main categories: brittle and ductile. Brittle materials, such as ceramics, fail with little to no plastic deformation, typically due to the rapid propagation of cracks. In contrast, ductile materials like metals undergo significant plastic deformation before failure, characterized by a gradual formation and growth of voids. When combining the two main categories, as in ceramic/metal bimaterials, the fracture behavior becomes more complex due to the differing mechanical properties of the two constituents. Ceramics contribute high stiffness and thermal resistance but are prone to brittle fracture, while metals offer ductility and toughness, providing resistance to crack propagation. The interface between these materials is often a critical zone where stress concentration and crack initiation occur, influenced by differences in thermal expansion, mechanical properties, and bonding strength. In ceramic/metal bimaterials, the fracture behavior is typically dominated by the weakest phase or the interface, with failure often occurring through delamination or crack deflection along the interface.

These advances are widely used in numerous industries and sectors, including aerospace, automotive, electronics, and energy. Their unique combination of high thermal stability, corrosion resistance, and mechanical strength makes them essential for components exposed to extreme environments, such as thermal barriers (Boissonnet et al., 2019; Yazdani & Isfahani, 2018; Bao et al., 2015), electronic packaging (Zhu et al., 2021; Zhang et al., 2015), and semiconductors (Adler et al., 2024).

* Corresponding author.
E-mail addresses: lamisse.tayeboun@univ-sba.dz (L. Tayeboun)

ISSN 2291-8752 (Online) - ISSN 2291-8744 (Print)
© 2026 Growing Science Ltd. All rights reserved.
doi: 10.5267/j.esm.2025.10.001

Over the past several years, various studies have focused on analyzing the interface in bimaterials (Drai et al., 2009; Lo et al., 1994; Chen, 1985; Marur & Tippur, 2000; Ouinas et al., 2012; Belhouari et al., 2011; Wang, 1998), and near the interface (Sérier et al., 1993; Boutabout et al., 2009),particularly the role it plays in fracture initiation and propagation. Researchers have examined factors such as interface adhesion, microstructural phenomena, defects (Farida et al., 2020),and residual stresses caused by thermal mismatches (Meyer & Schmauder, 1992), all of which significantly affect the material's fracture resistance. Current research continues to explore this area (Wang et al., 2022; Fu et al., 2023), investigating ways to enhance the bonding and fracture toughness of bimaterials, with particular attention to advanced materials and novel processing techniques that can improve the interface's reliability and performance.

The present work is part of this context, it aims to investigate the fracture mechanisms at the Alumina/Silver interface, particularly under mechanical, thermal, and thermo-mechanical loading conditions. By analyzing the Stress Intensity Factors (SIFs) across varying crack lengths, this study seeks to provide detailed insights into how different loading conditions influence crack propagation. Building on the micromechanical model proposed by (Farida et al., 2020), which examined defects at the metal-ceramic interface, this research adapts the same finite elements model. Still, it focuses on a crack positioned precisely at the interface between the two materials to model the mechanical response of the bimaterial interface under different loading scenarios. While this approach allows for a detailed analysis of stress distribution and SIFs, it is important to recognize that certain real-life factors, such as voids, grain boundary sliding, dislocation, and diffusion, can significantly affect fracture behavior. These factors were not integrated into the numerical model due to the complexity and limitations of simulating such microstructural phenomena. Nevertheless, the numerical results provide a foundational understanding of the stress patterns and crack propagation trends, which can later be enhanced through experimental studies or more advanced numerical models.

2. Materials And Methods

The Alumina/Silver bimaterial combines alumina's high hardness, thermal stability, and resistance to wear and corrosion with silver's superior electrical and thermal conductivity and flexibility. This yields a bimaterial with increased mechanical strength, effective thermal management, and resistance to thermal and mechanical stresses.

Table 1. Alumina (Al_2O_3) & Silver (Ag) Mechanical, Chemical and Physical Properties.

Properties	Alumina (Al_2O_3)	Silver (Ag)
Young's Modulus (GPa)	390	82
Poisson's ratio	0.25	0.31
Melting Point (K)	2345.15	1234.95
Thermal Expansion (K^{-1})	7.1×10^{-6}	19.6×10^{-6}
Thermal Conductivity (W/m·K)	30-35	429
Fracture Toughness (MPa√m)	3–5	40-105
Hardness (GPa)	15-19	3.25
Crystal Structure	Rhombohedral (Corundum)	Face-Centered Cubic (FCC)
Mechanical Behavior	Isotropic Elastic	Ductile (Plastic Deformation)

A three-dimensional model of an Alumina/Silver bimaterial, with dimensions of 350 µm in length and width, and 175 µm in thickness, was created to analyze bimaterial fracture behavior. A 2D schematic representation and a 3D geometry of the bimaterial model are presented in **(Fig. 1. (a-b))**. Alumina occupies 300 µm of the length, and silver the remaining 50 µm, forming a distinct interface. Pre-cracks, ranging from 10 to 100 µm, were introduced at the interface to study crack propagation under varying mechanical loads (uniformly distributed tensile loads with 70 to 160 MPa) and thermal loads (465.15–1138.75 K), as well as combined thermo-mechanical loads **(Fig. 1. (c))** .

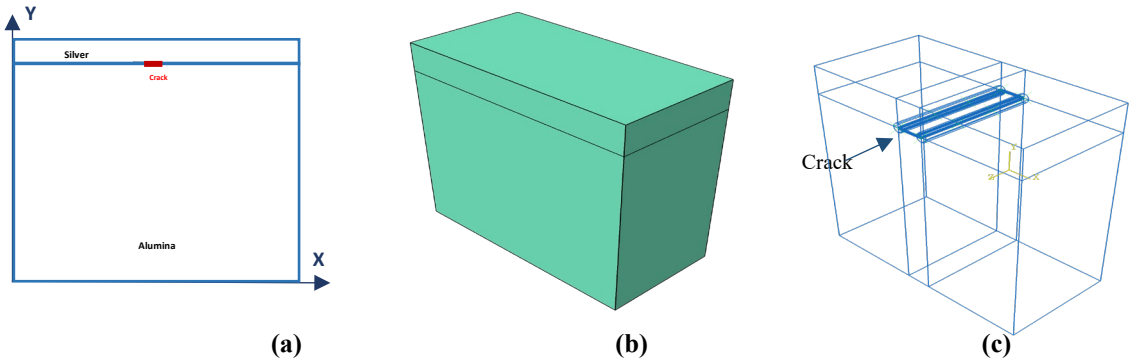

Fig. 1. (a) 2D schematic representation of the bimaterial configuration, (b) 3D geometry of the bimaterial model, (c) 3D view of the interfacial crack within the bimaterial structure

Finite element analysis (FEA) is used with Abaqus software, which provides a reliable platform for simulating stress distribution and intensity factors at fracture tips to evaluate fracture tendencies. A structured meshing strategy was employed to ensure high accuracy in the simulation results, especially around the crack tip and the interface between alumina and silver **(Fig. 2)**. Fine mesh elements were used in these critical areas to accurately capture the stress intensity factors (SIFs). The rest of the model was meshed with relatively coarser elements to reduce computational time without compromising the accuracy of the results.

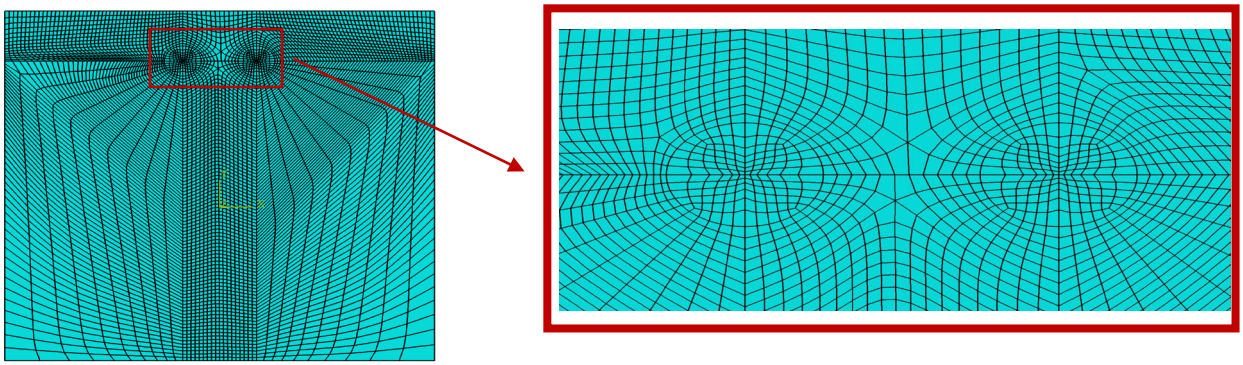

Fig. 2. Meshing Strategy and Crack Tip Refinement

Additionally, a mesh convergence study was performed to ensure that the results were independent of the mesh size **(Fig. 3)**.

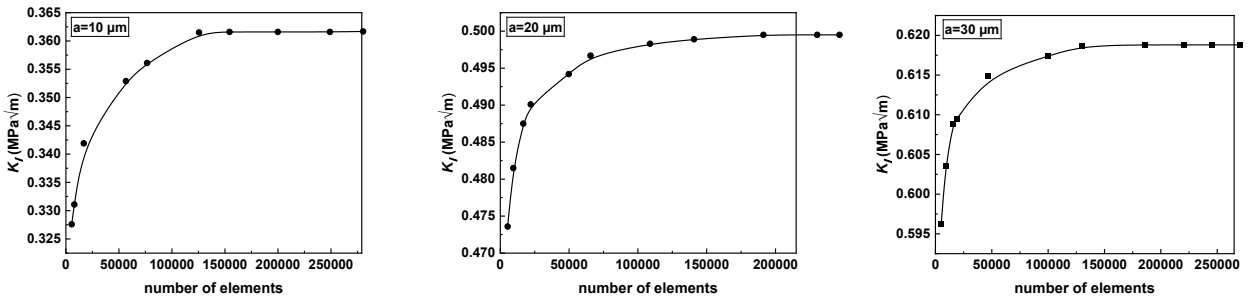

Fig. 3. Effect of mesh size convergence on bimaterial/crack interface

3. Results and Discussion

3.1 Effect of mechanical load

3.1.1 Effect of crack length

In the first case, we examine the mechanical effect of the Alumina/Silver bimaterial under a uniform tensile load of 70 MPa, focusing on the behavior of the bimaterial interface in the presence of pre-existing cracks ranging from 10 to 100 micrometers. The results depicted in **(Fig. 4)** demonstrate how the stress intensity factors (K_I, K_{II}, and K_{III}) evolve with crack length. K_I consistently increases as the crack length grows, suggesting that larger cracks make the opening mode stress intensity more significant. This trend can be directly associated with increased stress concentration at the crack tip, as longer cracks amplify the localized stresses, concentrating more energy at the fracture site.

The effect of the applied tensile load, which acts perpendicularly to the crack, further exacerbates this stress concentration at the crack tip. A load perpendicular to the crack surface causes an opening displacement of the crack faces, leading to the dominance of mode I fracture. This perpendicular load drives crack opening, contributing significantly to the rising K_I values. The applied stress intensifies near the crack tip, increasing the likelihood of crack propagation, especially in brittle materials like Alumina, where tensile stresses are less easily dissipated.

Notably, none of the K_I values exceed Alumina's fracture toughness range (K_{IC}), indicating that crack propagation remains controlled under a 70 MPa mechanical load. The relatively low values of K_{II} (ranging from 0.1 MPa√m to 0.18 MPa√m) suggest that sliding mode stresses contribute minimally to the overall fracture behavior, further emphasizing the dominance of K_I. Likewise, K_{III} values are negative, indicating a slight compressive tearing mode, with small absolute values (ranging from -0.04 MPa√m to -0.34 MPa√m), corroborating the minimal role of out-of-plane shear stresses in this context.

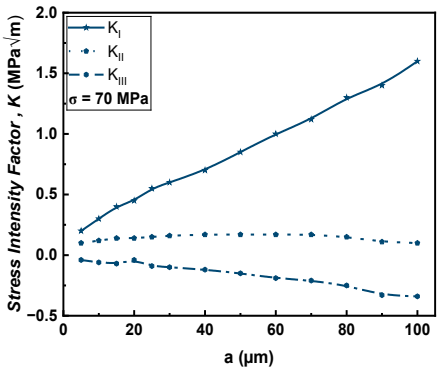

Fig. 4. Variation of Stress Intensity Factors (K_I, K_{II}, K_{III}) with Crack Length under Mechanical Loading (σ = 70 MPa)

To validate the numerical results, the following formulas were used to calculate stress intensity factors using Python software due to its efficiency in handling complex mathematical operations and optimizing computation time:

$$KI = YF\sigma(\sqrt{\pi a}) \tag{1}$$

The stress intensity factor, denoted as (K), is a fundamental parameter in fracture mechanics. It describes the stress state at a crack tip and is related to the rate of crack growth. George R. Irwin, often considered the father of fracture mechanics, developed the concept of the stress intensity factor in 1957 (Irwin, 1957).

$$Y = f(a/w) \tag{2}$$

$$Y = 1.12 - 0.231\left(\frac{a}{w}\right) + 10.55\left(\frac{a}{w}\right)^2 - 21.72\left(\frac{a}{w}\right)^3 + 30.39\left(\frac{a}{w}\right)^4 \tag{3}$$

where *Y* is called the geometry factor, signifying the geometry of a crack system in relation to the applied load. Normally, this geometry factor can be looked up in technical reference books. For a Centre crack in a finite-width strip, w, then the correction factor becomes a function of (a/w) (C. H. Wang, 1996).

F typically represents a correction or shape factor related to the specific geometry and loading conditions.

$$F = 1 + 0.5\left(\frac{E_1}{E_2}\right)\left(\frac{1-\nu_1^2}{1-\nu_2^2}\right) \tag{3}$$

The analytical results were then compared with the numerical values obtained from the finite element analysis, as shown in **(Fig. 5**). Both datasets follow a similar pattern, indicating a good correlation between numerical and analytical results. This consistency suggests that the numerical model can reliably estimate the stress intensity variables across varied crack lengths.

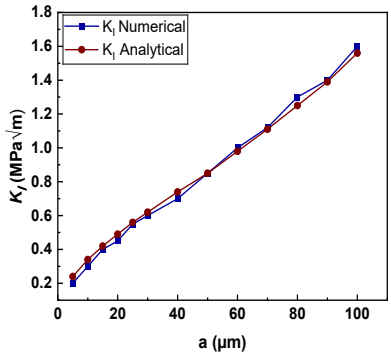

Fig. 5. Comparison of Numerical and Analytical K_I Values for Various Crack Lengths

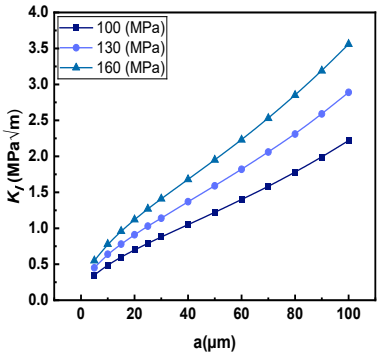

Fig. 6. Stress Intensity Factor KI for Different Tensile Loads: 100 MPa, 130 MPa, and 160 MPa

3.1.2 Effect of various mechanical loading

In the second case, we investigate the mechanical impacts on the Alumina/Silver bimaterial under increased uniform tensile stresses of 100 MPa, 130 MPa, and 160 MPa. At a mechanical load of 100 MPa, K_I increases from 0.1 MPa√m for a crack length of 5 µm to 2 MPa√m for 100 µm. Under a load of 130 MPa, K_I values are higher, starting at 0.2 MPa√m at 5 µm and reaching 2.5 MPa√m at 100 µm, with an increased risk of propagation for longer crack lengths. At 160 MPa, K_I significantly rises from 0.3 MPa√m to over 3 MPa√m, surpassing the lower limit of K_{IC} for cracks longer than 85 µm, suggesting probable propagation. These results indicate that higher mechanical loads elevate K_I, making longer cracks more susceptible to propagation, with the threshold for rapid crack growth between 130 MPa and 160 MPa. The plot illustrates how the stress intensity factor K_I varies with crack length under various loads **(Fig. 6)**.

3.2 Effect of thermal load

Understanding the influence of temperature on thermal expansion and Young's modulus is critical when analyzing the thermal effects on the behavior of the bimaterial. As a result, we first looked at how these properties changed with temperature for Alumina and Silver. The figures below show the variation of Young's modulus (Dickson & Wachtman, 1971; Smith & Fickett, 1995) and coefficient of thermal expansion (α) (Drai et al., 2009) **(Table 2)**

Table 2. Temperature Dependence of the Young's Modulus E of Alumina (Al_2O_3) (a) and Silver (Ag) (b)

Temp (K)	Temp	E (MPa)
298.15	25	390000
373.15	100	386708.4
473.15	200	382605.6
573.15	300	378163.5
673.15	400	373549.8
773.15	500	368826.9
873.15	600	364014.3
973.15	700	359147.1
1073.15	800	354233.1
1173.15	900	349237.2
1273.15	1000	344206.2

Temp (K)	Temp (C°)	E (MPa)	Temp (K)	Temp (C°)	E (MPa)
300.15	27	82,372	1050.15	777	58,372
350.15	77	80,772	1075.15	802	57,572
400.15	127	79,172	1100.15	827	56,772
450.15	177	77,572	1125.15	852	55,972
500.15	227	75,972	1150.15	877	55,172
550.15	277	74,372	1175.15	902	54,372
600.15	327	72,772	1200.15	927	53,572
650.15	377	71,172	1225.15	952	52,772
700.15	427	69,572	1250.15	977	51,972
750.15	477	67,972	1275.15	1002	51,172
800.15	527	66,372	1300.15	1027	50,372
850.15	577	64,772	1325.15	1052	49,572
900.15	627	63,172			
950.15	677	61,572			
1000.15	727	59,972			

To streamline the presentation of results and highlight key trends, we selected three representative crack lengths: 10 µm, 50 µm, and 100 µm. These lengths provide a comprehensive view of the behavior of the bimaterial under thermal effects by applying a temperature range from 465.15 K to 1138.75 K and capturing the response at short, medium, and long crack lengths. From the numerical analysis, two distinct behaviors were observed based on the location of the crack front. The distribution of residual stresses and their nature were not uniform along the crack front **(Fig. 7)**.

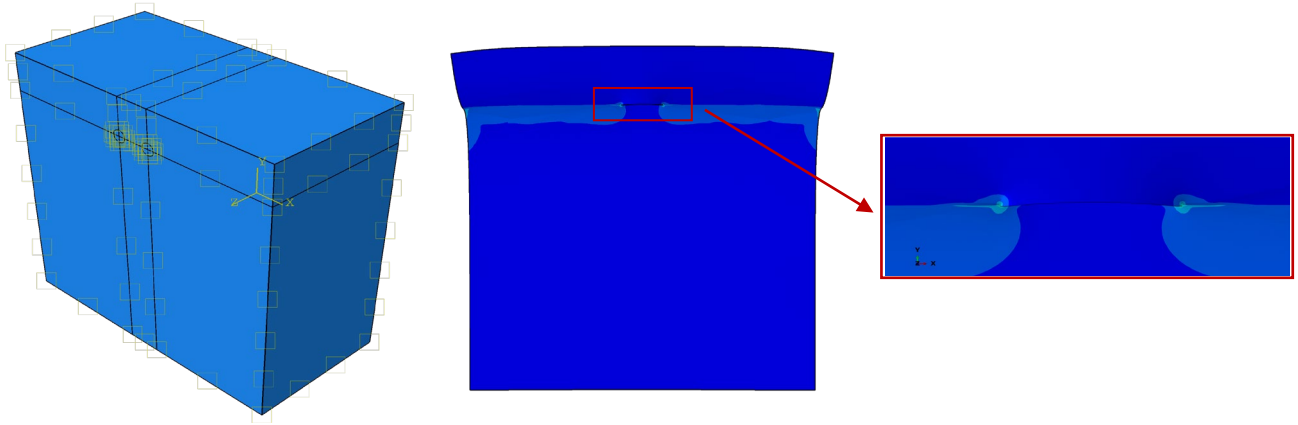

Fig. 7. Applied Thermal Conditions (a) and Resulting Crack Behavior (b) in the Bimaterial

Initially, at the surface of the bimaterial **(Fig. 8. (b)),** residual compressive stresses appear dominant, effectively closing the crack and reducing K_I. This behavior suggests that thermal stresses, driven by the mismatch in thermal expansion coefficients between Silver and Alumina, induce tensile stresses that counteract the compressive residual stresses present at the surface. The reduction in K_I at the surface, as temperature rises, further indicates that the thermal expansion-induced stresses are acting in a manner that helps close the crack, particularly near the surface. Minimal variation in K_{III} with

temperature suggests that the out-of-plane shear stresses are weak or balanced by residual compressive stresses, resulting in stable tearing mode stress intensity factors. A more complex trend was observed for K_{II} (Mode II - sliding mode): it generally increased for shorter cracks but either decreased or stabilized for longer cracks. This variation implies a complex interaction between thermally induced shear stresses and inherent residual stresses. Shorter cracks may be more susceptible to localized stress concentrations, while longer cracks experience a stabilization of these effects due to the redistribution of stresses along the crack front. As we move deeper into the bimaterial interface **(Fig. 8 (c))**, the results change significantly, and crack propagation becomes more pronounced, where tensile stresses dominate. The stress intensity factor K_I shows an increase with rising temperature across all crack lengths, a behavior attributed to the substantial tensile stresses at the interface caused by the differential expansion between the two materials. The mismatch in thermal expansion coefficients leads to tensile stresses within the interface, as Silver expands more than Alumina, generating higher stresses in the Alumina layer. This increase in K_I indicates that crack propagation is more likely at the interface, where the mismatch in both thermal expansion and Young's modulus between Alumina and Silver exacerbates stress concentrations and includes the rise of thermal stresses. On the other hand, K_{II} generally decreases within the interface, implying that the thermal shear stresses are oriented in a manner that mitigates the sliding mode stress intensity factor. Finally, K_{III} increases with temperature, particularly for longer cracks, indicating that the differential thermal expansion leads to more significant out-of-plane shear stresses, making the material more susceptible to tearing at the interface.

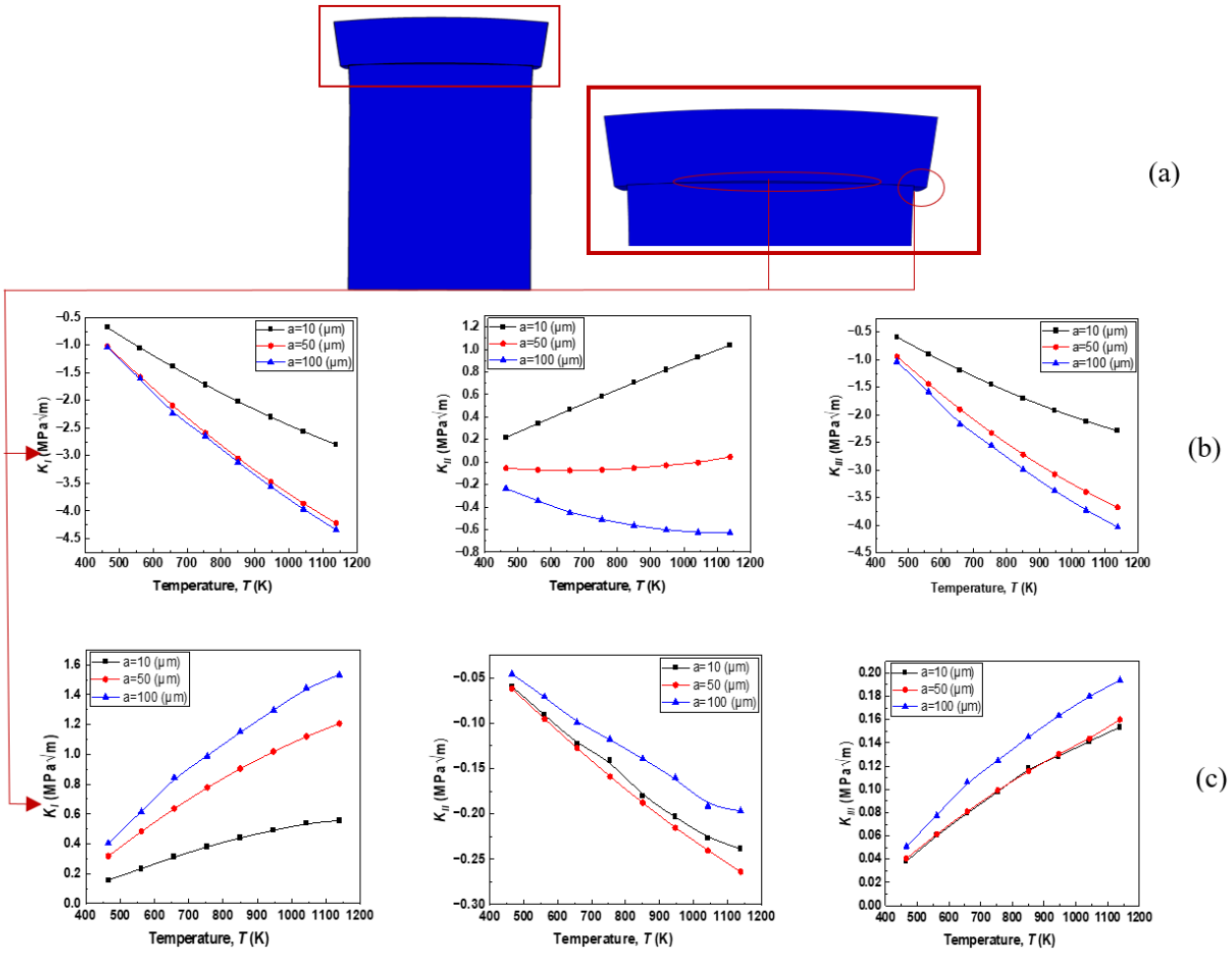

Fig. 8. Longitudinal Cross-Section of the Bimaterial Model (a) Temperature-Dependent Stress Intensity Factors K_I , K_{II}, and K_{III} at the Bimaterial Surface (b) and Interface (c) for Varying Crack Lengths.

3.3 Effect of thermo-mechanical load

This part of the research expands upon earlier investigations that isolated mechanical and thermal impacts, aiming to provide a comprehensive analysis of thermo-mechanical effects on stress intensity factors (SIFs). To effectively explore the combined effects of thermal and mechanical loading on the fracture behavior of Alumina/Silver bimaterial, this study strategically approaches the analysis in three distinct stages. Initially, the mechanical load is fixed at 130 MPa, accompanied by a temperature range from 465.506 K to 1138.75 K, focusing on various crack lengths, including 20 μm, 40 μm, 80 μm, and 100 μm and examining the behavior both at the surface and within the interior of the bimaterial **(Fig. 9)**. Comparative analysis of thermo-mechanical loading results **(Fig. 10)** with those from purely thermal loading **(Fig. 8)** reveals similar

patterns in SIF variations, with thermal effects predominantly influencing the material's response as temperature increases. At the surface **(Fig. 10 (b))**, K_I (Mode I - opening mode) decreases significantly with rising temperature, particularly for longer cracks. Similarly, K_{III} (Mode III) also decreases with temperature, indicating a diminished out-of-plane shear stress intensity, especially for longer cracks. This suggests that akin to purely thermal scenarios, the combined loading condition results in a reduced crack-driving force at the surface due to the thermal stress effect.

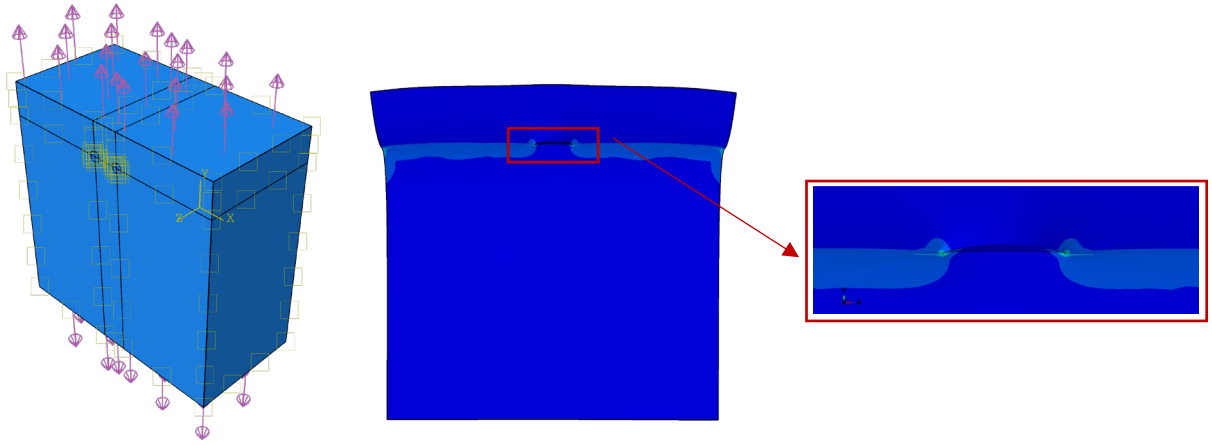

Fig. 9. Applied Thermo-mechanical Conditions (a) and Resulting Crack Behavior (b) in the Bimaterial

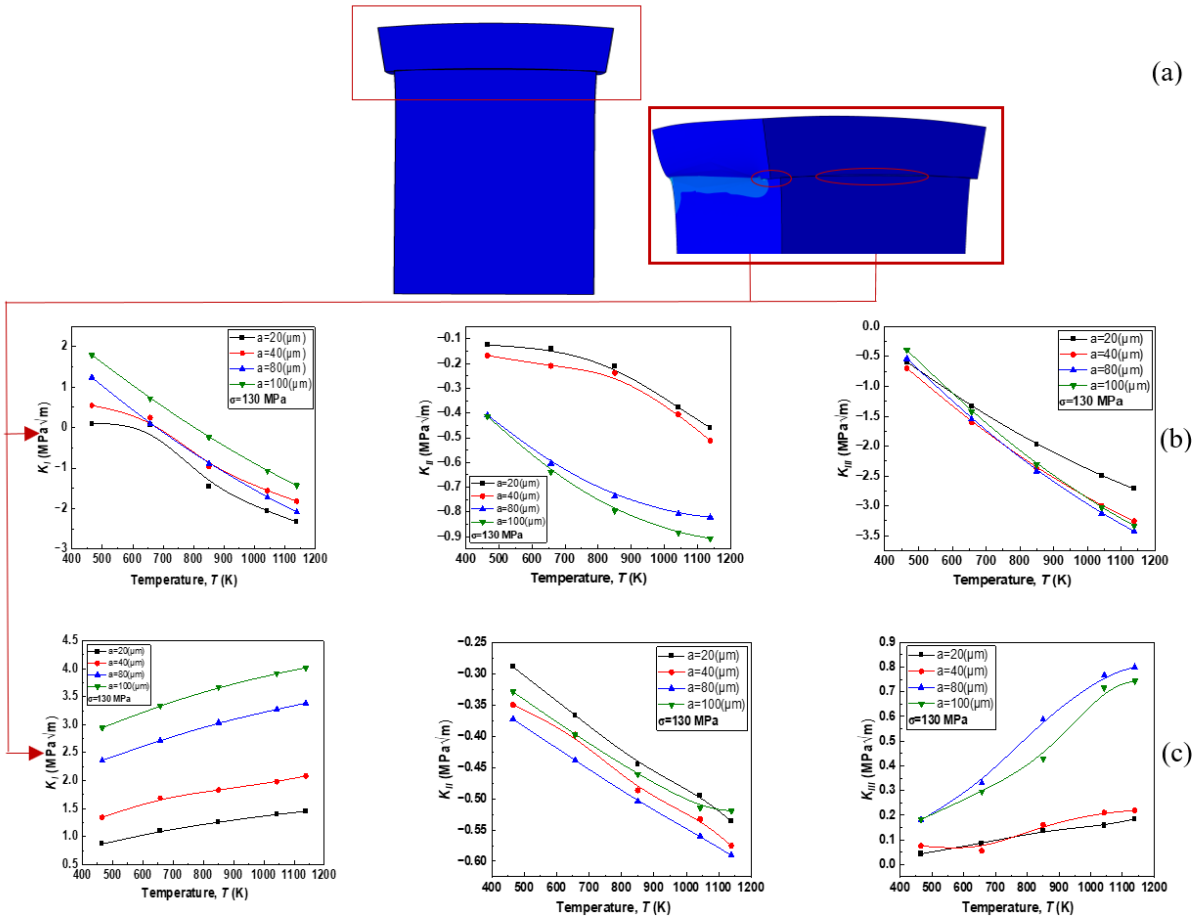

Fig. 10. Longitudinal Cross-Section of the Bimaterial Model (a) Surface (b) and interior (c) Stress Intensity Factor (SIF) Variations with Temperature under Fixed Mechanical Load (130 MPa).

Within the interface **(Fig. 10 (c))**, the findings mirror those of thermal loading, with increases in K_I and K_{III} as the temperature rises, especially for longer cracks. The thermal expansion mismatch between Alumina and Silver significantly generates residual tensile stresses in the interface, where the constraint from surrounding materials is greater. This mismatch in the mechanical properties of the two materials leads to a build-up of thermal stresses that enhance interfacial debonding and increase the likelihood of crack propagation. As K_{II} decreases in the surface and within the interface, it reflects a reduced shear stress intensity, particularly for longer cracks, indicating the intricate interplay of mechanical and thermal influences under these simulated operational conditions.

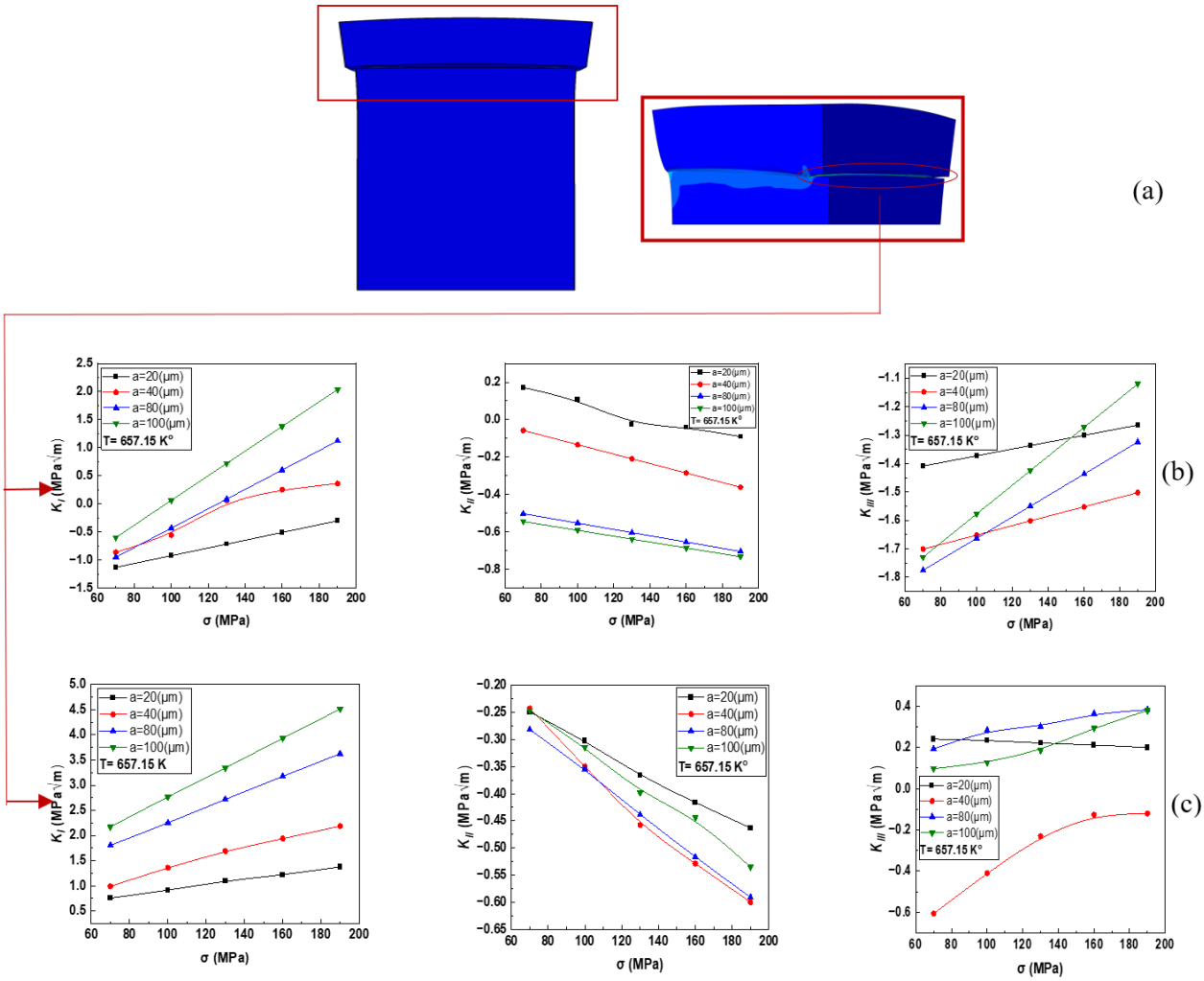

Fig. 11. Longitudinal Cross-Section of the Bimaterial Model (a) Surface (b) and interior (c) Stress Intensity Factor (SIF) Variations with Mechanical Load under Fixed Temperature (657.15 K).

In the second stage, the effects of a fixed temperature of 657.15 K and varying mechanical loads on the stress intensity factors (SIF) show distinct behaviors across different crack lengths at the surface and the interface **(Fig. 11 (a))**. At the surface **(Fig. 11 (b))**, the SIF in mode I (opening mode) increases linearly with the load for all crack lengths, indicating that the applied mechanical load directly influences the crack opening intensity. Conversely, mode II (sliding mode) shows a general decrease in SIF with increased load, suggesting that higher loads reduce in-plane shear stress, likely due to the crack opening. Mode III (tearing mode) SIF increases with the load, showing that the mechanical load reinforces out-of-plane shear stress. Similar trends are observed at the interface **(Fig. 11 (c))**, where mode I SIF increases linearly with the load, mode II SIF decreases, and mode III SIF increases across all crack lengths, highlighting consistent mechanical behavior within the bimaterial structure.

In the last stage, as the applied force increases from 100 MPa to 210 MPa and the temperature rises from 465.506 K to 1138.75 K, the combined thermomechanical effects on the bimaterial are evident **(Fig. 12)**. At the surface **(Fig. 12 (a))**, thermal effects start to play a more significant role, stabilizing K_I and K_{II} as temperature increases. Initially, mechanical loading drives the increase in K_I, but as the temperature rises, thermal effects counteract this, leading to a more stable K_I profile. The out-of-plane shear stress K_{III} shows minimal variation, indicating that it is less sensitive to the combined thermal and mechanical loading at the surface. In contrast, within the interface **(Fig. 12 (b))**, the stress intensity factors exhibit different behavior. K_I

is higher within the interface compared to the surface, reflecting greater stress concentration due to the combined effects of thermal expansion mismatch, thermal/tensile residual stresses, and mechanical loading. The K_{II} values also show more variations on the surface compared to the interface, suggesting that in-plane shear stress responses differ due to the surface's exposure. This difference underscores the stronger influence of thermal effects within the interface, where the higher mechanical and thermal stress concentrations lead to a more pronounced impact on the material's fracture behavior under combined loading conditions.

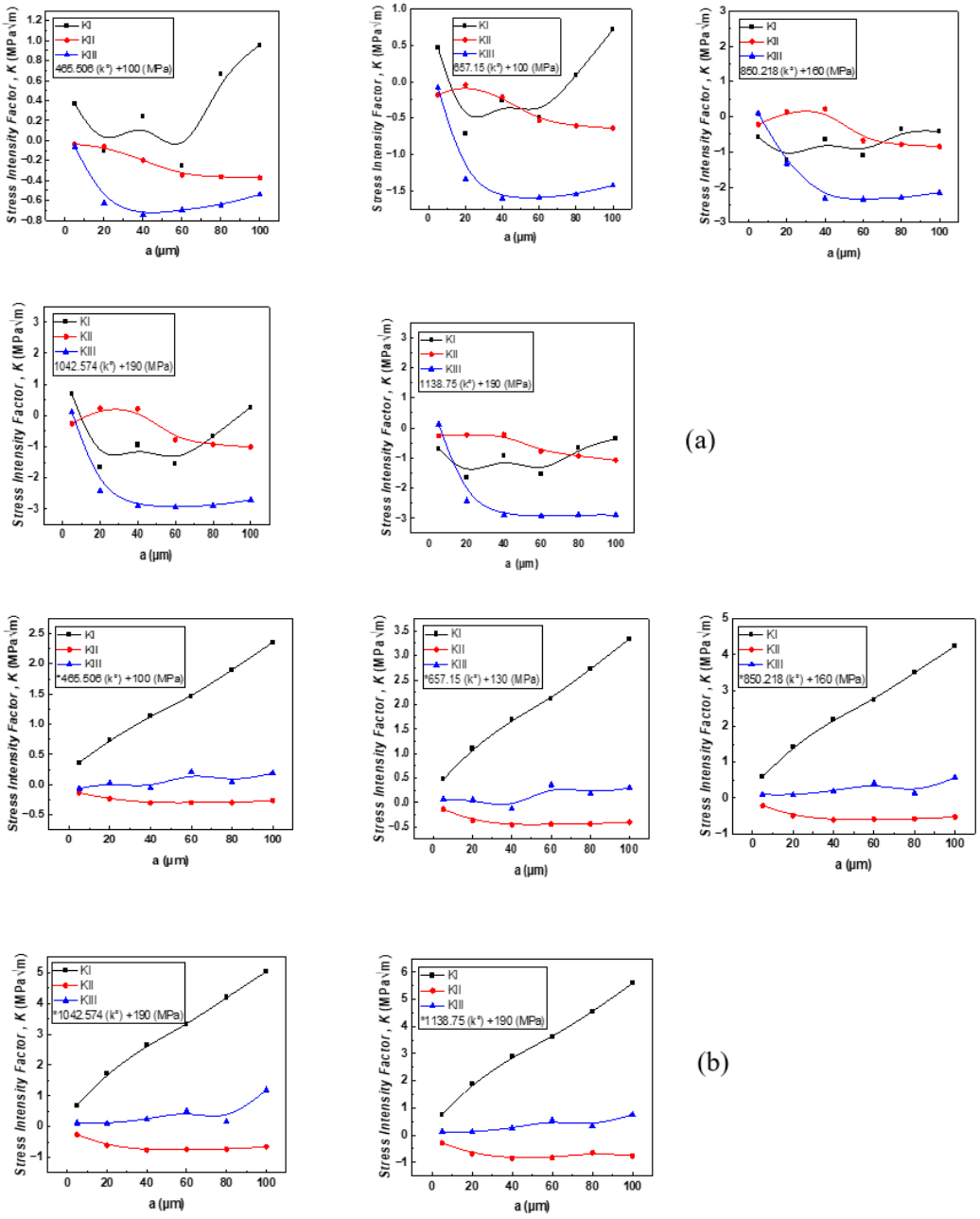

Fig. 12. Comparison of Stress Intensity Factors at the surface (a) and within the Interface (b) of the Bimaterial under Combined Thermomechanical Loads.

4. Conclusion

This study investigated the fracture behavior of Alumina/Silver bimaterials under mechanical, thermal, and combined thermo-mechanical loads, focusing on stress intensity factors (SIFs) K_I, K_{II}, and K_{III}. Results indicate that mechanical loading, especially in mode I, primarily drives crack propagation, with longer cracks concentrating stress at the tip. Thermal effects introduce complex behaviors, as surface cracks are stabilized by compressive stresses, while interface cracks experience increased propagation risk due to thermal expansion mismatches. Combined loading highlights that thermal effects have a more pronounced impact on SIFs, particularly within the interface, where stress concentrations intensify, promoting crack

growth. The findings underscore the importance of both mechanical and thermal contributions in understanding bimaterial fracture behavior.

References

Adler, C., Morais, P., Akhavan-Safar, A., Carbas, R. J. C., Marques, E. A. S., Karunamurthy, B., & Da Silva, L. F. M. (2024). Cohesive Properties of Bimaterial Interfaces in Semiconductors: Experimental Study and Numerical Simulation Using an Inverse Cohesive Contact Approach. *Materials*, *17*(2), 289.

Bao, Z., Guo, X., & Shang, F. (2015). An atomistic investigation into the nature of fracture of Ni/Al2O3 interface with yttrium dopant under tension. *Engineering Fracture Mechanics*, *150*, 239–247.

Belhouari, M., Bouiadjra, B. B., Kaddouri, K., & Achour, T. (2011). Plasticity Effect on Crack Growth along Ceramic/Metal Bimaterial Interface: Numerical Analysis. *Mechanics of Advanced Materials and Structures*, *18*(5), 364–372.

Boissonnet, G., Bonnet, G., Pasquet, A., Bourhila, N., & Pedraza, F. (2019). Evolution of thermal insulation of plasma-sprayed thermal barrier coating systems with exposure to high temperature. *Journal of the European Ceramic Society*, *39*(6), 2111–2121.

Boutabout, B., Chama, M., Bouiadjra, B. A. B., Serier, B., & Lousdad, A. (2009). Effect of thermomechanical loads on the propagation of crack near the interface brittle/ductile. *Computational Materials Science*, *46*(4), 906–911.

Chen, E. P. (1985). Finite element analysis of a bimaterial interface crack. *Theoretical and Applied Fracture Mechanics*, *3*(3), 257–262.

Dickson, R. W., & Wachtman, J. B. (1971). An alumina standard reference material for resonance frequency and dynamic elastic moduli measurement. I. For use at 25 C. *Journal of Research of the National Bureau of Standards Section A: Physics and Chemistry*, *75A*(3), 155.

Drai, A., Bouiadjra, B. B., Meddah, M., & Benguediab, M. (2009). Analysis of interfacial fracture in ceramic–metal assemblies under effect of thermal residual stresses. *Computational Materials Science*, *46*(4), 1119–1123.

Farida, B., Hadid, L., Boualem, S., & Sikandar, S. (2020). Finite element analysis of the interface defect in ceramic-metal assemblies: Alumina-Silver. *Fracture and Structural Integrity*, *14*(53), 1-12.

Fu, X., Liang, L., & Wei, Y. (2023). Characterization and Simulation of Nanoscale Catastrophic Failure of Metal/Ceramic Interfaces. *ACS Omega*, *8*(23), 20313–20322.

Irwin, G. R. (1957). Analysis of Stresses and Strains Near the End of a Crack Traversing a Plate. *Journal of Applied Mechanics*, *24*(3), 361–364.

Lo, C. Y., Nakamura, T., & Kushner, A. (1994). Computational analysis of dynamic crack propagation along a bimaterial interface. *International Journal of Solids and Structures*, *31*(2), 145–168.

Marur, P. R., & Tippur, H. V. (2000). Dynamic response of bimaterial and graded interface cracks under impact loading. *International Journal of Fracture*, *103*(1), 95–109.

Meyer, M., & Schmauder, S. (1992). Thermal stress intensity factors of interface cracks in bimaterials. *International Journal of Fracture*, *57*(4), 381–388.

Ouinas, D., Sahnoun, M., & Benderdouche, N. (2012). FE Analysis of Sif of Interfacial Crack Emanating from a Circular Notch in Ceramic/Metal Bi-Materials. *Advanced Materials Research*, *428*, 121–126.

Sérier, B., Berroug, A., Juvé, D., Tréheux, D., & Moya, E. G. (1993). Silver-alumina solid state bonding: Study of diffusion and toughness close to the interface. *Journal of the European Ceramic Society*, *12*(5), 385–390.

Smith, D. R., & Fickett, F. R. (1995). Low-Temperature Properties of Silver. *Journal of Research of the National Institute of Standards and Technology*, *100*(2), 119.

Wang, C. H. (1996). *Introduction to Fracture Mechanics*. Defence Science and Technology Organisation.

Wang, J.-S. (1998). A micromechanical model for interface crack extension in metal/ceramic bimaterial systems. *Acta Materialia*, *46*(14), 4973–4984.

Wang, X., Gu, Y., & Golub, M. V. (2022). Analysis of bimaterial interface cracks using the localized method of fundamental solutions. *Results in Applied Mathematics*, *13*, 100231.

Yazdani, A., & Isfahani, T. (2018). Hardness, wear resistance and bonding strength of nano structured functionally graded Ni-Al2O3 composite coatings fabricated by ball milling method. *Advanced Powder Technology*, *29*(5), 1306–1316.

Zhang, Z., Long, Y., Cazottes, S., Daniel, R., Mitterer, C., & Dehm, G. (2015). The peculiarity of the metal-ceramic interface. *Scientific Reports*, *5*(1).

Zhu, Q., Pan, Z., Zhao, Z., Cao, G., Luo, L., Ni, C., Wei, H., Zhang, Z., Sansoz, F., & Wang, J. (2021). Defect-driven selective metal oxidation at atomic scale. *Nature Communications*, *12*(1).

© 2026 by the authors; licensee Growing Science, Canada. This is an open access article distributed under the terms and conditions of the Creative Commons Attribution (CC-BY) license (http://creativecommons.org/licenses/by/4.0/).